



Study on Deformation Mechanism and Stability Analysis of Mined-Out Areas in Small Coal Mines

Xufeng Zhuang*, Xiao Yu, Chengyang Mao, Shiyu Yi and Aibin Cao

Research Center of Applied Geology of China Geological Survey, Chengdu, Sichuan, 610036, China

*Corresponding author's e-mail: xfz0379@126.com

Abstract. The mined-out areas of small coal mines are characterized by strong concealment and irregular distribution, and the deformation and failure mechanisms of overlying rock and soil masses in these areas present significant technical challenges for stability analysis in surface engineering construction. Through theoretical analysis and field investigations combined with engineering practices in small coal mine goaf areas, this study explores deformation mechanisms and stability analysis methods. Research indicates that the deformation of small coal mine goaf areas results from the combined effects of multiple factors, including the ratio of mining depth to thickness, dip angle of overlying strata, and hydrogeological conditions. Based on the deformation patterns of overlying strata in mined-out areas, a stability evaluation method integrating classical limit equilibrium theory calculations with numerical simulations was proposed. By coupling the maximum residual deformation value and conducting deep ground displacement monitoring, the cumulative maximum deformation remains below the maximum residual deformation threshold. These research outcomes provide theoretical foundations and practical guidance for stability analysis in engineering construction within small coal mine goaf areas, demonstrating significant engineering application value.

Keywords: Mined-out area; Deformation mechanisms; Stability analysis; Limit equilibrium; Numerical simulation

1 Introduction

When conducting engineering construction around coal-rich towns, it is inevitable to encounter small coal mine goaf areas requiring treatment. These areas present urgent challenges in accurately identifying mining depth and thickness, as well as in conducting mechanistic analyses of the failure mechanisms of overlying rock masses and calculating their stability. In recent years, scholars have increasingly focused on research related to small coal mine goaf areas. In the field of goaf investigation, Cai Weiyi et al. studied the application of integrated geophysical methods for goaf detection^[1], while Sun Jin et al. identified goaf distribution through seismic wave analysis and drilling verification^[2]. In stability analysis, Zhang Xin et al. refined standardized formulas by

directly converting the loose layer into bedrock thickness^[3] at a certain ratio before substituting it into the formula for calculation.

Currently, there is limited research on the deformation mechanisms and patterns of small coal mine goaf areas. Therefore, this paper, based on engineering case studies, analyzes the deformation characteristics of goaf areas, summarizes deformation patterns, and explores rational and applicable evaluation methods as well as safe and cost-effective treatment measures for small coal mine goaf areas.

2 Deformation Characteristics of the Study Area

The coal-bearing strata in the study area belong to the Upper Permian Xuanwei Formation (P_3x) and the second member of the Emeishan Basalt Formation ($P_3\beta$). The Xuanwei Formation contains 15 workable coal seams, including 10 seams minable across the entire area (Nos. 3, 10, 12, 15, 16, 17, 18, 24, 26, and 27) and 5 seams minable in most regions (Nos. 1, 5, 6, 23, and 29). The Emeishan Basalt Formation contains 1 workable coal seam (No. 32), with others being minable in most regions. The physical properties of these coal seams vary slightly. They are predominantly black to grayish-black in color, with structures dominated by blocky or granular textures and locally stratified layers. The luster is primarily vitreous, with some exhibiting submetallic sheen. Fracture surfaces show conchoidal breaks, partially irregular. The coal exhibits banded structures, some with linear textures, and a massive structure. The coal is hard and brittle in nature.

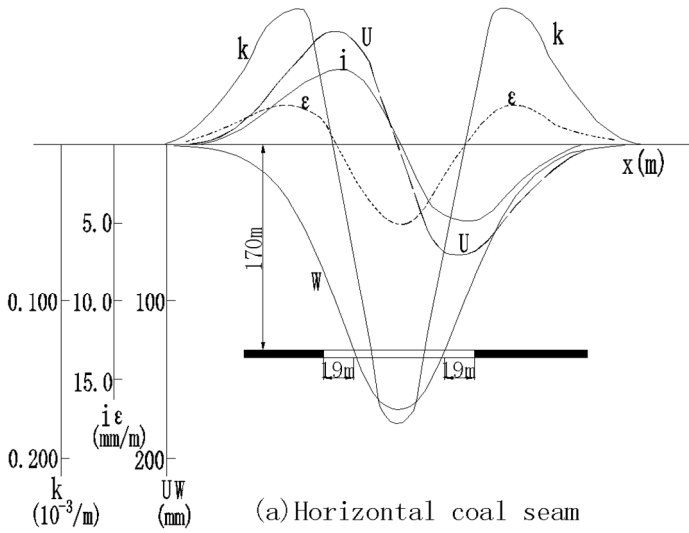
The engineering construction site contains 7 coal mine tunnels, resulting from unauthorized and disorderly mining by local villagers between 1960 and 1990, with some tunnel entrances now sealed and buried. These tunnels have widths of 1.2–2 m, heights of 1.5–2.5 m, and depths ranging from 20 to 150 m. The mining directions are irregular, with interconnected and intersecting coal seam excavations.

Within the site, a small coal mine goaf destruction zone has formed, spanning approximately 345 m in length and 150–250 m in width. The goaf areas are buried at depths ranging from 10 to 70 m (confirmed by multiple boreholes during drilling investigations). Water accumulation is observed in the entrances of tunnels MD3–MD7, with groundwater flowing out of the openings. The goaf areas have caused surface damage and subsidence deformation.

3 Deformation Mechanism Analysis of Overlying Strata in Small Coal Mine Mining

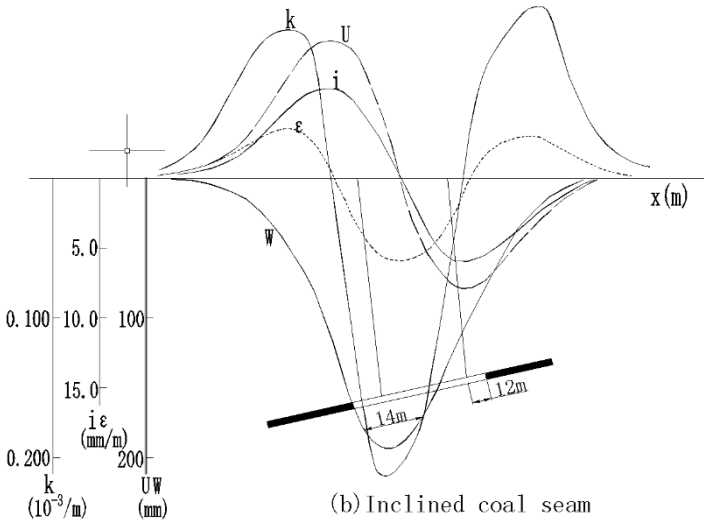
From the perspective of rock mechanics, the fundamental mechanism of overlying rock and soil layer deformation in small coal mine goaf areas lies in the disruption of the static equilibrium of the rock mass caused by underground coal mining. This disturbance triggers stress redistribution in the surrounding rock of mining tunnels, leading to unloading deformation, which subsequently propagates upward and manifests as surface cracks and sinkholes. The entire deformation process is influenced by multiple

factors, primarily including the ratio of mining depth to thickness, properties of overlying strata, dip angle of coal seams, exposure duration, and hydrogeological conditions.



W-Sink; i-Incline; k-Curvature; U-Horizontal movement; ϵ -Horizontal deformation

Fig. 1. Deformation of horizontal coal seam.



W-Sink; i-Incline; k-Curvature; U-Horizontal movement; ϵ -Horizontal deformation

Fig. 2. Deformation of inclined coal seam.

Numerous domestic and international studies^[4] have focused on exploring the functional relationships between surface deformation in goaf areas and the ratio of mining depth to thickness (H/T) as well as the dip angle of coal seams. Analytical studies suggest that under these two variables, the movement and deformation of overlying strata in small coal mine mining exhibit certain regularities.

When the H/T ratio in small coal mine goaf areas is less than 10, the overlying strata generally undergo brittle failure, resulting in intense and discontinuous surface deformation characterized by scattered subsidence pits or fractures. Conversely, when the H/T ratio exceeds 10, the overlying strata tend to form three collapse zones (caving, fractured, and continuous deformation zones). Surface movement and deformation in both horizontal coal seams (Figure 1) and inclined coal seams (Figure 2) demonstrate spatial and temporal continuity and predictability.

4 Stability Assessment of Mined-Out Zones in Artisanal Coal Mines

4.1 Geotechnical Parameters and Model Boundaries

Based on the exploration data, the small coal mine primarily extracted the shallow No. 1 coal seam with a gentle dip angle. The goaf tunnels have widths of 1.2–2 m and heights of 1.5–2.5 m, exhibiting linear alignment. The overlying rock-soil strata above the goaf tunnels consist sequentially of 12 m-thick mudstone and 35 m-thick sandstone. The applied load in the study area is considered to be 180 kPa.

To accurately analyze the deformation of the overlying rock-soil mass in the goaf area of the study region, four key parameters were selected for the overlying strata and coal seams: unit weight (γ), compressive strength (σ), Young's modulus (E), and Poisson's ratio (λ). These parameters are summarized in Table 1.

Table 1. Parameters of each layer of rock and soil mass.

Rock	γ /(KN/m ³)	σ /(MPa)	E/(GPa)	λ
Sandstone	26.2	29.8	24.5	0.3
Mudstone	24.4	11.4	12.3	0.3
Coal seam	21.5	4	3	0.3

4.2 Limit Equilibrium Analysis Method

Based on the static equilibrium condition and the Mohr-Coulomb strength criterion, the limit equilibrium method assesses the stability of the overlying rock mass and the site foundation by calculating the ratio of the anti-sliding force to the sliding force on the sliding surface, known as the safety factor (Fs).

Roof Stability Calculation:

$$h_{cr1} = \frac{2a}{tg \phi \times tg^2(45^\circ - \frac{\phi}{2})}$$

ϕ : Weighted internal friction angle of overlying strata

a : Half of the tunnel width

Foundation Stability Calculation:

$$h_{cr2} = \frac{B \times \gamma + \sqrt{B^2 \times \gamma^2 + 4 \times B \times \gamma \times P \times t g \phi \times t g^2 (45^\circ - \frac{\phi}{2})}}{2 \times \gamma \times t g \phi \times t g^2 (45^\circ - \frac{\phi}{2})}$$

ϕ : Weighted internal friction angle of overlying strata

B : Tunnel width

γ : Weighted unit weight of overlying strata

P : Surface load

Stability Criteria: Unstable foundation: $h < h_{cr}$; Poor stability: $h_{cr} \leq h \leq 1.5 h_{cr}$; Stable foundation: $h > 1.5 h_{cr}$. Calculated critical heights: $h_{cr1} = 0.5\text{m}$, $h_{cr2} = 15.4\text{ m}$; Actual thickness of overlying strata: $h = 47\text{ m}$; Conclusion: The foundation in the study area is stable.

4.3 Numerical Analysis

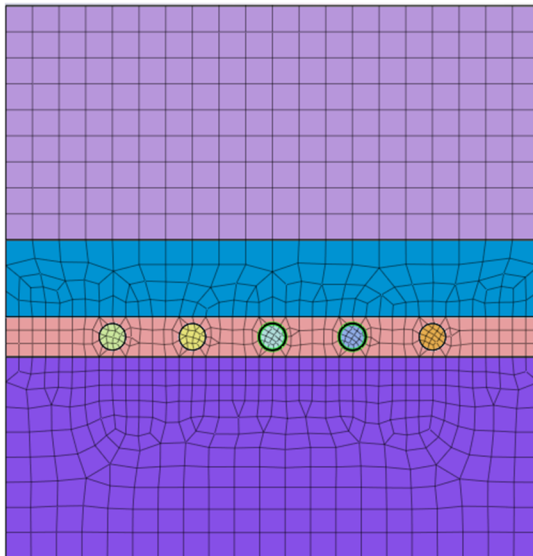


Fig. 3. Numerical Calculation Model Grid Division.

The principle of the numerical method is based on borehole data and geological profiles to construct a fundamental model. Irregular cavities were defined using production records, and random joint sets were generated through a discrete fracture network (DFN) with a lognormal spacing distribution^[5]. When the equivalent plastic strain (p) reaches or exceeds 0.02, the element is removed to simulate collapse and strength reduction. The material strength parameters are gradually decreased (c reduction = c/F , \tan reduction = $(\tan \phi)/F$) until the model fails to converge^[6], at which point F represents the

safety factor. This study involves a multi-scale coupling analysis of the stability of mined-out areas in small coal kilns.

Numerical simulations were conducted using MIDAS-GTS software. A three-dimensional computational model was established based on the actual terrain and the spatial distribution of the underlying goaf (mined-out area). The model dimensions were set as follows: longitudinal length= 100 m, transverse width= 26 m, and vertical height= 80 m (Figure 3).

After coal tunnel excavation and without considering surface loads, the overlying rock mass formed a caving zone under self-weight due to mining-induced disturbances. The maximum displacement occurred within three times the tunnel diameter (3D). Given the thick sandstone overburden above the coal tunnel, the natural collapse propagated upward to the ground surface, resulting in a vertical surface displacement of 2.32×10^{-3} m (Figure 4).

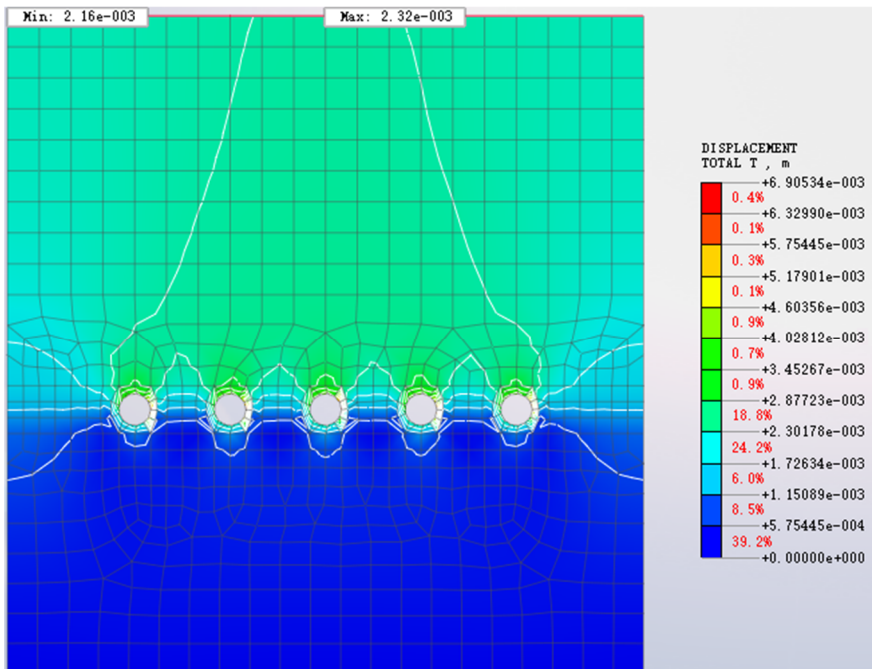


Fig. 4. Vertical displacement of overlying rock before filling.

The vertical displacement of the overlying strata above the coal tunnel under engineering fill was simulated. Under the combined action of the applied load (180 kPa) and the self-weight of the overlying strata, the resulting vertical ground surface displacement reached 7.40×10^{-2} m (Figure 5).

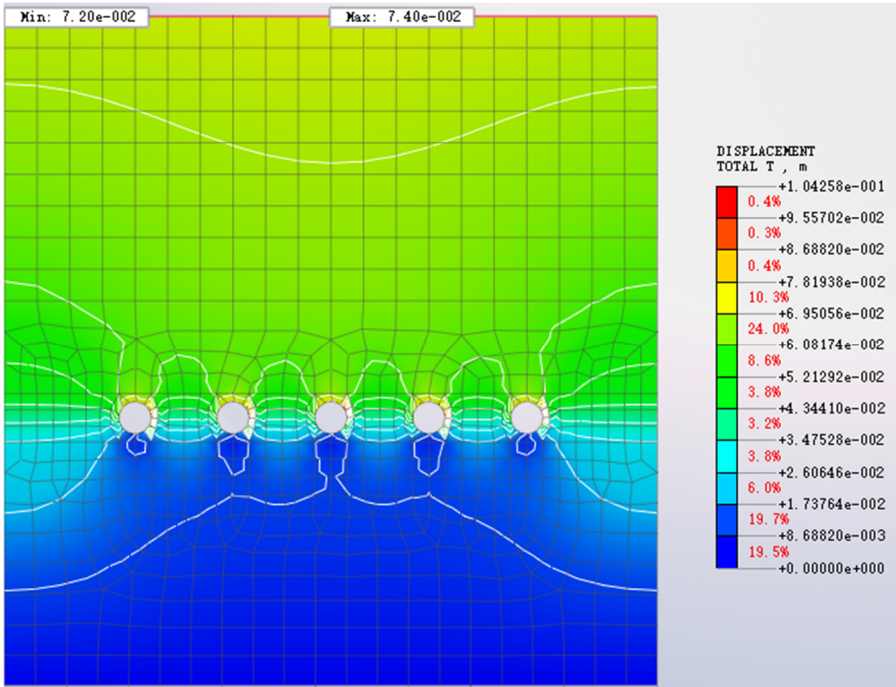


Fig. 5. Vertical displacement of overlying rock after filling.

The simulation results indicate that the vertical displacement of the foundation in the study area after fill placement is 7.40×10^{-2} m, which meets the deformation requirements for stable goaf sites. By synthesizing the results of the limit equilibrium analysis method and numerical simulations, the study area exhibits favorable stability and is suitable for engineering construction.

5 Subgrade Monitoring Analysis

Based on the stability evaluation conclusions for the goaf area, which indicated favorable site stability, the study area underwent direct engineering fill after dynamic compaction treatment. The embankment section reached its design elevation in May 2022. Four deep-seated displacement monitoring points were installed diagonally across the site. By August 2023, 15 datasets had been collected, and the monitoring data were processed to plot the deep vertical displacement curves (Figure 6).

Analysis of the settlement-time curves reveals that during the monitoring period: Initial deformation increments at all monitoring points exhibited non-uniform growth rates.

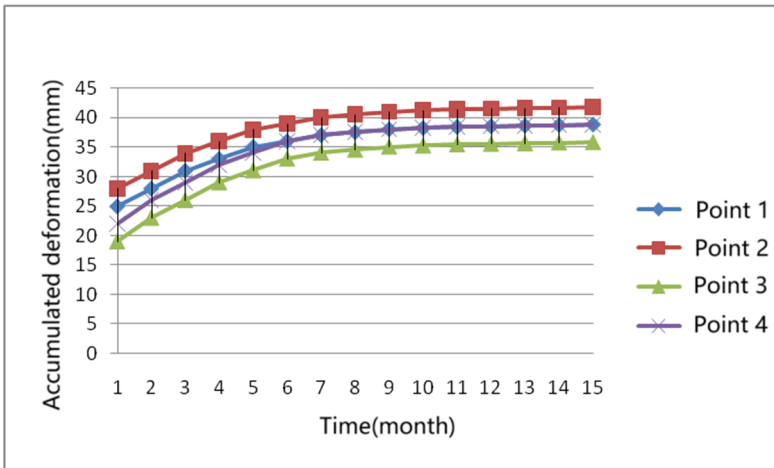


Fig. 6. Deep vertical displacement curve.

After 9 months, cumulative vertical displacements stabilized, indicating the roadbed foundation settlement had entered the residual deformation phase.

Final cumulative vertical displacements at 15 months:

D1: 38.8 mm, D2: 41.2 mm, D3: 35.7 mm, D4: 39.8 mm

All values fell within codified limits (e.g., ≤ 50 mm per 《Technical Code for Highway Subgrades》 JTG D30-2015). Monitoring data validated the reliability of the coupled theoretical and numerical analytical methodology.

6 Conclusions

1) The key factors controlling the movement and deformation of overlying strata in small coal mine goaf areas can be categorized into five primary parameters: the mining depth-to-thickness ratio, overburden properties, coal seam dip angle, exposure duration, and hydrogeological conditions. Among these, the mining depth-to-thickness ratio governs the spatial extent of surface subsidence by regulating the development height of overburden failure zones, while the coal seam dip angle influences the directional failure pattern of rock masses through stress field deflection. Together, these two parameters create a dual-parameter control equation for predicting ground movement.

2) For goafs with mining depth-to-thickness ratios < 10 , overlying strata typically undergo brittle failure, resulting in intense discontinuous surface deformations such as scattered subsidence depressions or fissures. For ratios > 10 , strata deformation resembles that of large-scale mining areas, forming caving zones.

3) The limit equilibrium method efficiently quantifies the safety factor and shear reserve of a roof using static equilibrium and the Mohr-Coulomb criterion. By constructing a three-dimensional elastoplastic model, the numerical analysis method can accurately simulate fracture propagation and the multi-field coupling effects of overburden rock. Together, these two approaches form a complementary system of

qualitative screening and quantitative analysis, effectively distinguishing the stability of overburden rock in mined-out areas of small coal mines.

4) The research findings offer technical support for engineering construction in small coal mine goaf areas. However, due to limitations in sample size and regional scope, future applications of the computational methods necessitate an expanded statistical analysis of deformation patterns using larger sample sizes.

Acknowledgments

This work was supported by China Geological Survey Project [NO. DD20230133].

References

1. Cai W, Zhang D and Tao X (2019) Suitability analysis of railway route selection in coal mine goaf areas. *J. Coal Engineering*, 51(2): 124–129.
2. Sun L (2020) Engineering geological investigation and stability evaluation of small coal mine goafs. *J. Railway Investigation and Surveying*, 5: 85–90.
3. Zhang F and Dong W (2018) Analysis of stability factors in small mine goafs based on numerical simulation. *J. Chinese Journal of Underground Space and Engineering*, 14: 935–939.
4. Zuo H, Zha J and Lin W (2019) Integrated survey technology for shallow small coal mine goafs beneath mountain highways. *J. Western China Communications Science & Technology*, 10: 51–54.
5. Shi W, Cui P and Xue F (2019) Mining-induced deformation characteristics and stability evaluation of substations in small coal mine goafs. *J. Shanxi Architecture*, 8: 47–48.
6. Wang Y and Mao X (2013) Stability analysis methods for goafs beneath highway bridges. *J. Highway*, 10: 93–96.

Open Access This chapter is licensed under the terms of the Creative Commons Attribution-NonCommercial 4.0 International License (<http://creativecommons.org/licenses/by-nc/4.0/>), which permits any noncommercial use, sharing, adaptation, distribution and reproduction in any medium or format, as long as you give appropriate credit to the original author(s) and the source, provide a link to the Creative Commons license and indicate if changes were made.

The images or other third party material in this chapter are included in the chapter's Creative Commons license, unless indicated otherwise in a credit line to the material. If material is not included in the chapter's Creative Commons license and your intended use is not permitted by statutory regulation or exceeds the permitted use, you will need to obtain permission directly from the copyright holder.

